Research Article

Kang Yang*#, Yong Yang#, Ji Wang, Xinyue Fan, Dongqing He, and Zan Lv

Low-velocity impact response optimization of the foam-cored sandwich panels with CFRP skins for electric aircraft fuselage skin application

https://doi.org/10.1515/secm-2024-0021
received February 06, 2024; accepted May 22, 2024

Abstract: Composite sandwich structures are widely used in the aerospace field due to their advantages of high strength, lightweight, and fatigue resistance. However, these structures are prone to damage with very-low-energy impacts. In order to improve the impact resistance of aircraft skin structure, a low-velocity impact resistance of sandwich structure specimens was tested by means of drop hammer impact, and the impact damage area was scanned by ultrasonic C-scan, and obtains the impact damage of specimens with different impact energies and different ply sequences. Combined with the Hashin failure criterion, the finite element equivalent model of composite sandwich structure under low-velocity impact was established. The errors between the simulation results and the C-scan results of the test piece were less than 10%, in which the experimental measurements and numerical predictions were in close agreement. Finally, the finite element equivalent model was applied to optimize the application of model sandwich, which was used for fuselage skin of a certain electric aircraft. The total thickness of the laminate structure remains unchanged before and after optimization, but the impact resistance was significantly enhanced. The ±45° layup was beneficial for the structure to absorb the impact energy.

Keywords: impact resistance, sandwich structure, ultrasound C-scan, low-velocity impact, finite element analysis

1 Introduction

Electric aircraft has irreplaceable advantages such as environmental friendliness, easy maintenance, and low operating cost. However, compared with oil-powered aircraft, electric aircraft still has many shortcomings in terms of maximum range and maximum flight time. The demand for advanced materials and structural design is more urgent [1–3]. The sandwich structure has become an effective way to lighten aircraft and has been widely used in the aviation field due to its high specific strength, good stability, corrosion resistance, and structural design ability [4–7]. However, in daily use and maintenance processes, it is often subjected to low-energy impacts from various external objects such as hail and maintenance tools, which is easy to cause a significant decline in performance. Therefore, it is necessary to study the damage of the sandwich structure after low-speed impact. With the aggravation of the greenhouse effect, electrified aircraft is a promising solution to combat the aviation greenhouse gas challenge [8–10]. In order to reduce the energy consumption of electric aircraft, electric aircraft needs to use lightweight and efficient composite structures [11–13]. Impact failure is a common problem that affects the strength and structural integrity of sandwich composites [14,15]. This issue is usually caused by the degradation of energy absorption competence and structural stiffness. The sandwich structure suffers major damage from the impact load, and the damage progressively increases with repeated loading [16,17]. Therefore, hybrid composites are designed and developed to improve different properties such as impact resistance, joining inserts, bending, and perforation behavior [18–23].

With rapid advance in numerical techniques represented by finite element method, it becomes feasible to precisely simulate impact process of sandwich structures.

# Yong Yang and Kang Yang have contributed equally to this work.

* **Corresponding author: Kang Yang,** Design Department, Liaoning General Aviation Academy, Shenyang, China; College of Aerospace Engineering, Shenyang Aerospace University, Shenyang, China, e-mail: ykangok@163.com
Yong Yang: Consulting Div, WISDRI Iron & Steel Engineering & Research Incorporation Limited, Wuhan, 430223, China
Ji Wang, Xinyue Fan, Dongqing He: Design Department, Liaoning General Aviation Academy, Shenyang, China
Zan Lv: Design Department, Liaoning General Aviation Academy, Shenyang, China

Zhu *et al.* [24] investigated the influence of impact position and impact energy on the post-impact compressive strength of composite panel honeycomb sandwich structures through experiments and simulations, compared two typical impact characteristics of maximum impact force and displacement, and revealed the relationship between impact position and post-impact compressive strength. Xiao *et al.* [25] used polyvinyl chloride foam as material to experiment and simulate the repeated dynamic mechanical behavior of foam core sandwich plate. It is a valuable analysis method for the prediction of structural plastic deformation and cumulative damage under repeated impact and provides a possible way for the design of foam–core sandwich structure against repeated impact. Jianfeng *et al.* [26] conducted experimental and numerical studies on the dynamic response and failure of carbon fiber-reinforced plastic Kagome lattice core sandwich panels under low-velocity impact. The results showed that the dynamic response and energy absorption of the sandwich plate are sensitive to the impactor size and impact position. In addition, researchers all over the world have carried out many studies on the low-energy impact of the sandwich structures [27–32]. Valerio *et al.* [27] united the ability of composite materials with innovative additive manufacturing processes and performed numerical sensitivity analysis on the impact response of polypropylene and composite sandwich structures with different skin and honeycomb core thicknesses at an impact load of 20 J. Moreover, mechanical responses of different sandwich shock absorbers was compared and a minimum-mass configuration that maximises energy absorption was identified Besant *et al.* [28] analytically investigated low-velocity impact responses and crashworthiness of different face sheets and foam–core sandwich structures. To further improve their impact resistance, some researchers introduced the density gradient of graded foam as a core in the sandwich panel, finding that the negative density gradient of core assuredly improves the energy absorption capability of the panel [29,30]. Zhu and Sun [31] developed an energy-based analytical model for multilayer sandwich panels to predict contact force, impact displacement, and energy absorption.

In this study, the finite element equivalent model of composite sandwich structure under low-velocity impact was established based on the Hashin failure criterion. The numerical simulation was applied to the structural optimization design of an electric aircraft, providing theoretical basis and data support for the design of composite electric aircraft.

2 Materials and methods

The specimens of this test were sandwiched structure formed by carbon fiber-reinforced polymer (CFRP) composites and lightweight foam. The face sheets were made of carbon fiber-woven fabric reinforced in epoxy resin, in which each play thickness was 0.125 mm and using wet molding process, brand W-3021FF (manufacturer: Weihai Guangwei Composite Materials Co., Ltd.). The core material selected a polyurethane foaming plastic for this research work, with material grade being H60 (manufacturer: Kunshan Daibo New Material Co., Ltd.) and cross-sectional thickness of 4 mm. The composite foam sandwich panel belongs to a three-layer bonding structure, which was formed by hand pasting and vacuum bag pressing technology. The panel and foam are bonded with epoxy resin glue. The entire composite sandwich test piece after forming was cut into typical impact test pieces with a length of 150 mm × 100 mm. The dimensions and structural schematic diagram of the test pieces are shown in Figure 1. After all the test pieces were cut off, subsequent mechanical tests and inspections were carried out. The detailed information of the test piece is shown in Table 1.

The test was carried out in accordance with American society for testing material D7136 standard. A steel drop hammer was introduced to carry out low-energy impact on the sandwich plate. The diameter of the punch was 20 mm, the weight of the whole hammer was 5.5 kg, and the ambient temperature/humidity was 25°C/40% RH. The test piece was tightened by the chuck on the edge, and the

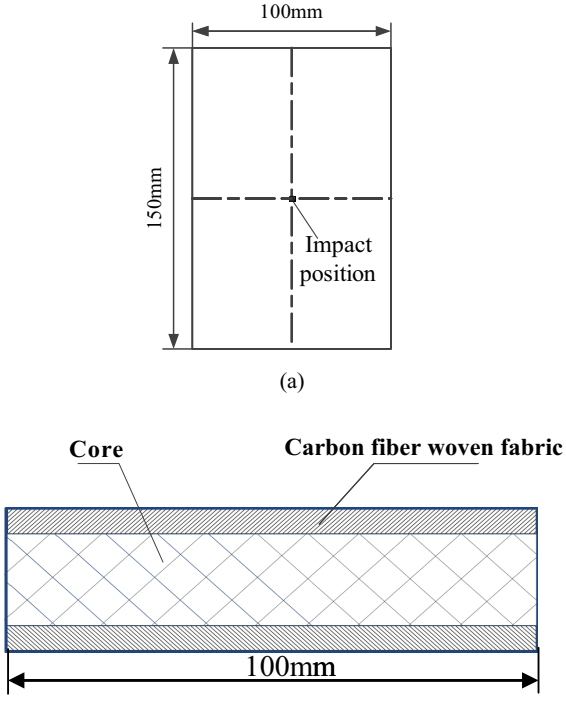

Figure 1: Schematic diagram of standard specimen dimensions and impact position (mm): (a) schematic diagram of sample size and impact position and (b) schematic diagram of sample structure form.

Table 1: Test piece laying method and impact energy

Specimen notation		Sandwich panel-laying sequence	Sandwich height (mm)	Energy level (J)
San-A	San-A01	[±45°/(core)/±45°]	4.5	10.58
	San-A02			21.17
	San-A03			31.75
	San-A04			42.34
San-B	San-B01	[±45°/(0°,90°)/(core)/±45°]	4.75	10.58
	San-B02			21.17
	San-B03			31.75
	San-B04			42.34
San-C	San-C01	[±45°/(0°,90°)(core)/(0°,90°)/±45°]	5	10.58
	San-C02			21.17
	San-C03			31.75
	San-C04			42.34
San-D	San-D01	[±45°/±45°/(core)/±45°/±45°]	5	10.58
	San-D02			21.17
	San-D03			31.75
	San-D04			42.34

impact energy reached 10.58, 21.17, 31.75, and 42.34 J by manually adjusting the height of the hammer head. Multiple test pieces were used for each test group to ensure the accuracy of the test results. Each test piece was a single impact. Ultrasonic C-scan (SAM300 Basic, German PVATePla Company) was used to detect the impact damage characteristics, as shown in Figure 2.

3 Result of experiment and numerical simulation

3.1 Low-velocity impact test and results

Under the energy of 21.17 J, the ultrasonic C-scan results of impact damage depth and damage surface diameter of different layup test pieces are shown in Figure 3. It can be seen that under the same impact energy, the depth and area of the impact damage area of each group of test pieces change with the number of layers and laying angle of the woven cloth. Under different impact energies, the data of damage depth and damage diameter (surface) of each group of specimens are shown in Table 2. According to the experimental data, it can be seen that the variation pattern of impact damage depth and area of the test piece was the same under different impact energies. As the impact energy increased, the depth and diameter of the impact damage area of the test piece gradually increased.

The specimen San-B adopted an asymmetric layered structure, while San-A, San-C, and San-D were symmetrical layered structures. Comparing the damage situation of specimen San-B with that of specimens San-A, San-C, and San-D, the results showed that the surface damage shape of

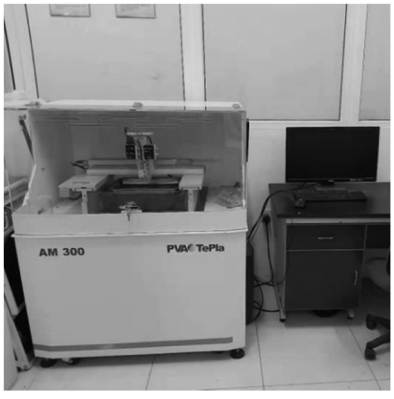

(a)

(b)

Figure 2: Test equipment and process: (a) ultrasonic scanning system and (b) drop hammer impact testing machine.

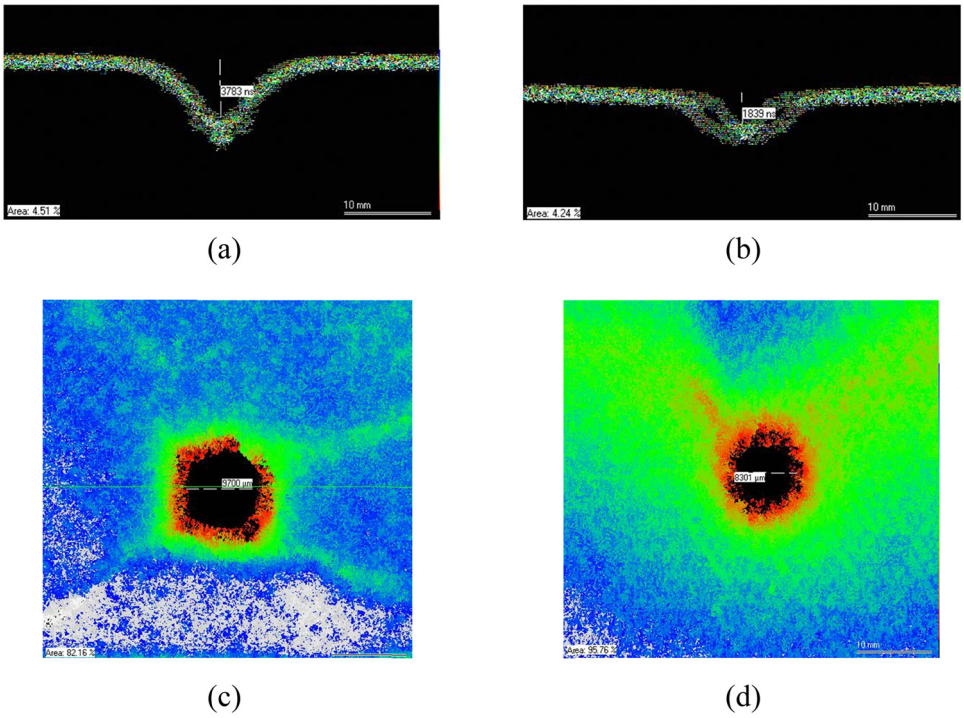

Figure 3: Typical electron microscope C-scan image of area damage at different impact energies: (a) damage depth of specimen San-A02, (b) damage depth of specimen San-C02, (c) damage diameter of specimen San-A02, and (d) damage diameter of specimen San-C02.

specimen San-B was irregular, while the surface damage shape of specimens with other symmetrical layers tended to be more circular; under different energy impacts, the damage areas of samples in the San-A, San-C, and San-D groups were all smaller than those in the San-B group; from this, it can be concluded that asymmetric layering will reduce its impact resistance. This was because during the curing process, the mismatch in the thermal expansion coefficient between the layers of the asymmetric layering has caused the rectangular sandwich panel to deform into an arch shape under the action of thermal stress, and the diameter damage on the surface of the specimen will be more severe. The specimens San-A, San-C, and San-D all adopt symmetrical layered structures. Compared the damage situation of specimen San-A with that of specimens San-C and San-D, the results showed that under the same impact energy, the depth damage of San-A was smaller, but the damage diameter on the damage surface was the largest; analyzing the experimental results, it was found that under the same energy, the more carbon fiber layers are arranged in the specimen, the greater the depth of damage and the smaller the diameter of the damage surface. This was because the fibers in each layer of the woven fabric layer sample were interwoven and arranged with each other, and there were interweaving points, so the anti-layering ability increased with the increased fiber arrangement. When the impact energy increased to 42.34 J, the depth of damage in San-C and San-D was greater and the specimen was completely penetrated. However, due to the interlacing of more fibers, the crack propagation to a larger range was effectively suppressed. The impact energy

Table 2: Comparison table of low-velocity impact deep damage test and simulation results

No.	Impact energy (J)	Damage depth (mm)	Damage diameter (μm)	Value of simulation (mm)	Error value (%)
San-A01	10.58	1.18	6,200	1.25	5.93
San-A02	21.17	1.51	9,700	1.58	4.64
San-A03	31.75	1.71	11,400	1.73	1.17
San-A04	42.34	2.21	14,800	2.43	9.95
San-B01	10.58	1.75	10,800	1.78	1.71
San-B02	21.17	3.04	15,700	2.79	8.22
San-B03	31.75	3.36	16,400	3.54	5.36
San-B04	42.34	—	16,801	—	—
San-C01	10.58	2.38	7,303	2.47	3.78
San-C02	21.17	3.72	8,101	3.88	4.31
San-C03	31.75	—	11,500	—	—
San-C04	42.34	—	12,302	—	—
San-D01	10.58	1.3	5,500	1.39	6.92
San-D02	21.17	1.57	6,600	1.61	2.55
San-D03	31.75	1.62	8,300	1.66	2.47
San-D04	42.34	2.14	11,300	2.15	0.47

was concentrated near the impact point, so the diameter of the damage surface was much smaller than that of San-A. San-A lacks more fiber layout, and the main form of damage was delaminated, with fewer fiber fractures along the thickness direction. Comparing the San-C and San-D test pieces, the damage of San-D was smaller under the same impact energy; when the impact energy does not exceed 21.71 J, there is no significant damage to the sandwich test pieces of the two layering sequences; after the impact energy reached 31.75 J, the anti-impact load capacity of the sandwich test piece with sandwich structure of San-C significantly decreased, while the anti-impact performance of San-D was better.

3.2 Finite element simulation and comparative analysis

The impact simulation model was established in Abaqus 6.12 using the lamination method and size data of impact specimens. The impact position was the center of the model, and the thickness of the middle core material foam was 4 mm. The failure model of the carbon fiber panel was a two-dimensional Hashin failure model, and the elastic parameter type of the carbon fiber material was a Lamina model. The main performance parameters of the composite panel and the foam–core material are shown in Tables 3 and 4. The simulation type was EXPLICIT display analysis. The upper and lower panels of the model were simulated by the 8-node quadrilateral plane continuous shell element SC8R to simulate the carbon fiber panel, which can effectively reduce the hourglass integration; the foam–core material was determined as isotropic material, and the eight-node hexahedral C3D8R solid element modeling of linear reduction integral element was used; the impact head was set as a rigid body, the elastic modulus was 210 GPa, the Poisson's ratio was 0.3, the mass was set as 5.5 kg by adjusting the density, and the unit type was C3D8R solid element. The impact height of the drop hammer in the test was replaced by the equivalent kinetic formula, and the initial velocity of the punch was 1.961, 2.775, 3.398, and 3.923 m/s, corresponding to the impact energy of 10.58, 21.17, 31.75, and 42.34 J. The comparison diagram of the typical finite element numerical simulation results of the specimen and the damage of the panel in the impact test is shown in Figure 4. The damage effects of the two are nearly X-shaped, breaking along the punch to the peripheral fibers, and obvious damage is seen at the upper end, and the fracture areas of the two are consistent.

In order to verify the effectiveness of this model in predicting the low-speed impact response and impact loss of composite foam sandwich panels, the damage depth and surface damage diameter of the test pieces measured by ultrasonic C-scan were compared with the finite element numerical simulation results. The process of finite element simulation is that the punch starts from contacting the panel, the velocity becomes zero, and then, the punch rebounds from the sandwich panel until the specimen was stable. Considering the elastic properties of the foam, the impact force on the panel is analyzed, and the impact damage is reflected by the deformation of the overall model when the impact force changes from low to high and then to zero. The comparison between the finite element simulation and C-scan results of the damage zone is shown in Figure 5. The damage position of the test piece was the direct contact position of the punch. In the finite element model, the upper panel of carbon fiber composite material is directly impacted, and the panel damage is only in the local area near the impact

Table 3: Physical parameters of punch

Radius r (mm)	Height h (mm)	Mass m (kg)	Density ρ_2 (kg/m^3)
10	20	5.5	875.06

Table 4: Performance parameters of composite sandwich panel

Performance parameters of composite panel				Performance parameters of foam core material	
Parameter type	Value	Parameter type (MPa)	Value	Parameter type	Value
E_1(GPa)	147.22	X_T	2527	Density (g/cm^3)	0.06
E_2(GPa)	8.05	X_C	969.64	Shear strength (MPa)	0.76
G_{12}(GPa)	4.05	Y_T	41.69	Shear modulus (MPa)	21
G_{13}(GPa)	4.05	Y_C	167.22	Tensile strength (MPa)	1.8
G_{23}(GPa)	3.67	S_L	106.87	Tensile modulus (MPa)	75
v_{12}	0.32	S_T	106.87	Compressive strength (MPa)	0.9
—				Poisson's ratio	0.37

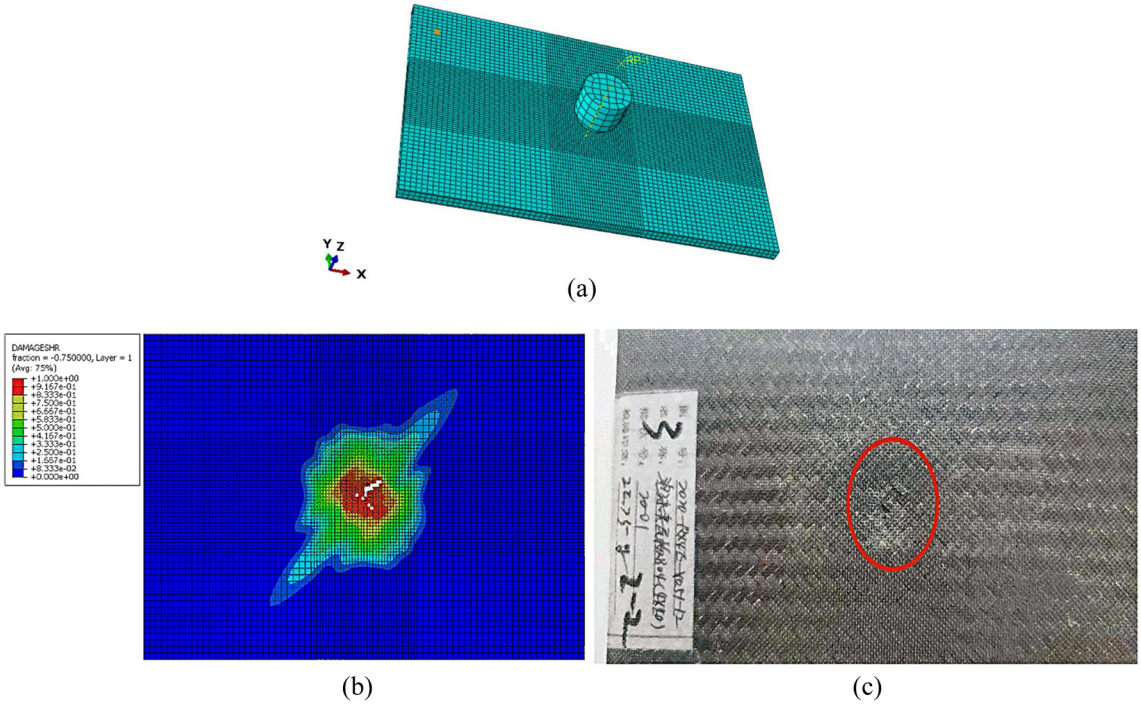

Figure 4: Diagram of damage comparison of the upper panel of the specimen of San-D02: (a) model meshing, (b) finite element analysis results, and (c) testing results.

position. The comparison of finite element simulation and C-scan results of damage depth and surface damage diameter is shown in Table 2. From the comparison of data in the table, it can be seen that the composite sandwich plate model and compressible foam model theory used in this article can well simulate the damage process of carbon fiber composite foam plate under low-speed impact. The error between the depth damage simulation and the test value in the remaining cases was less than 10%, except for the complete penetration of several groups of data.

4 Finite element analysis of composite foam sandwich fuselage skin

4.1 Simplified finite element model

Based on the aforementioned test and analysis results, this study took the outer fuselage of an electric aircraft as the

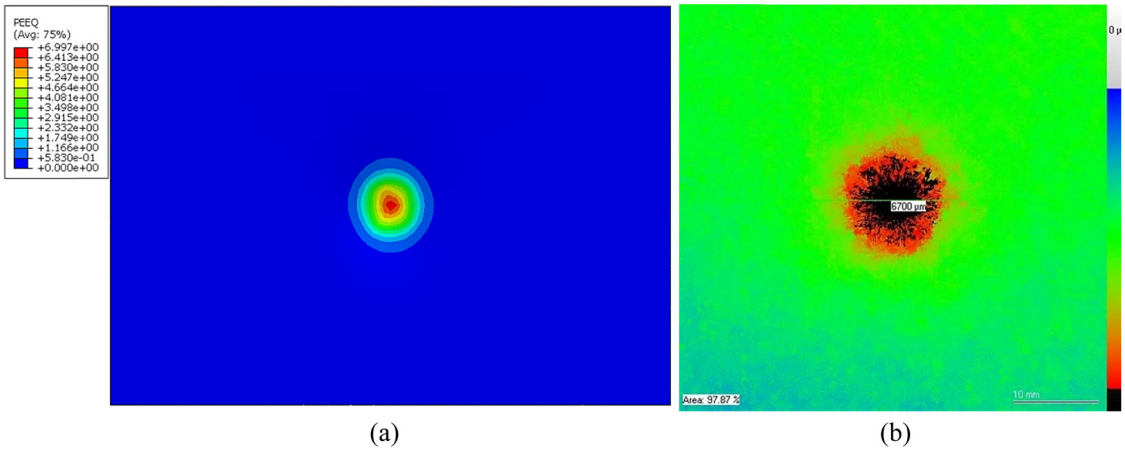

Figure 5: Typical diagram of damage area comparison of the specimen of San-D02: (a) finite element analysis results and (b) ultrasonic C-scan results.

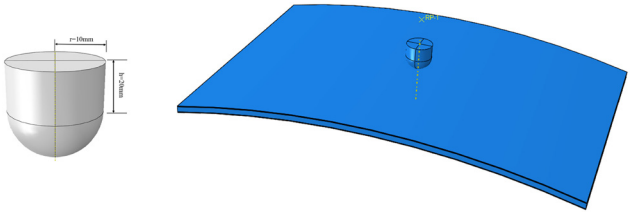

Figure 6: Schematic diagram of punch geometric model and impact model.

research object and selected a 300 mm × 200 mm fuselage skin for equivalent low-speed impact simulation calculation in Abaqus. The skin was a composite material foam sandwich structure, with fixed support boundaries set around the periphery, and the impact position was the center of the curved panel. The analysis type was EXPLICIT display analysis. The upper and lower panels were W-3021FF composite laminates, the parameter model was the Hashin failure criterion, and the unit type was continuous shell unit SC8R modeling. The intermediate foam sandwich was H60 rigid polyvinyl chloride foam, isotropic, and the unit type was C3D8R solid modeling. The material parameters and performance are shown in Table 3. The impact model is shown in Figure 6, and the radius of curvature was 300 mm.

The impact object was replaced by a hemispherical cylinder punch model with a radius of 10 mm. The punch starts to be perpendicular to the center of the impacted surface, and the vertical downward initial velocity was 2.7 m/s, equivalent to 20 J impact energy. The contact between impact structures was defined as surface-to-surface contact, and the friction coefficient was set to 0.2. The deformation of the impactor was not considered in this simulation. The punch was made of rigid material and set as a rigid body. The linear elastic constitutive model was adopted, and its parameters are shown in Table 4.

In this study, the impact resistance of fuselage skin was optimized from the carbon fiber laminate structure. Based on the aforementioned test and simulation results, the impact damage of sandwich parts was reduced by changing the ply angle and proportion of upper and lower panels. The before and after optimization impact results were compared and analyzed to prove the rationality of optimization. The panel properties before and after optimization are shown in Table 5.

4.2 Impact response analysis

Figure 7 is the cloud chart of the plastic deformation and displacement deformation of the sandwich foam before and after the optimization of the sandwich skin. It can be seen from the figure that the plastic deformation of the foam takes place in the area directly contacted by the punch, the deformation range was approximately oval and evenly and symmetrically distributed along the impact point, the deformation displacement of the foam causes deep damage along the impact center, and the foam mainly collapses. According to the numerical analysis and comparison of YHR and YH3 ply structures, the plastic deformation range of sandwich skin in full ply [(0°, 90°)] direction was the largest, and the depth displacement deformation was large, while the plastic deformation range of sandwich skin in full ply [(±45°)] direction was the smallest, and the depth displacement deformation was small.

Figure 8 shows the change of overall energy before and after ply optimization. Among them, E_K represents the kinetic energy of the punch at the beginning of the impact process, E_I represents the change of the overall internal energy of the sandwich structure during the impact process, E_{DMD} represents the damage dissipation energy during the impact process, and E_{PD} represents the plastic dissipation energy during the impact process. The energy of E_{DMD} and E_{PD} indicated the overall damage of the sandwich panel. The greater the corresponding energy value, the more serious the damage of the structure. The thickness of the sandwich parts before and after optimization was the same, and the response time of the four ply structures in the impact process is also basically the same. The final kinetic energy of YHR before optimization is 7661 mJ, while the kinetic energy of YH1, YH2, and YH3 is 9,066, 10,643, and

Table 5: Laying scheme of fuselage skin sandwich parts

	No.	Laminate composites	Thickness (mm)
Before optimization	YHR	[(0°,90°)/(0°,90°)/(0°,90°)/(core)/(0°,90°)/(0°,90°)/(0°,90°)]	5.5
After optimization	YH1	[±45°/(0°,90°)/(0°,90°)/(core)/(0°,90°)/(0°,90°)/±45°]	5.5
	YH2	[±45°/±45°/(0°,90°)/(core)/(0°,90°)/±45°/±45°]	5.5
	YH3	[±45°/±45°/±45°/(core)/±45°/±45°/±45°]	5.5

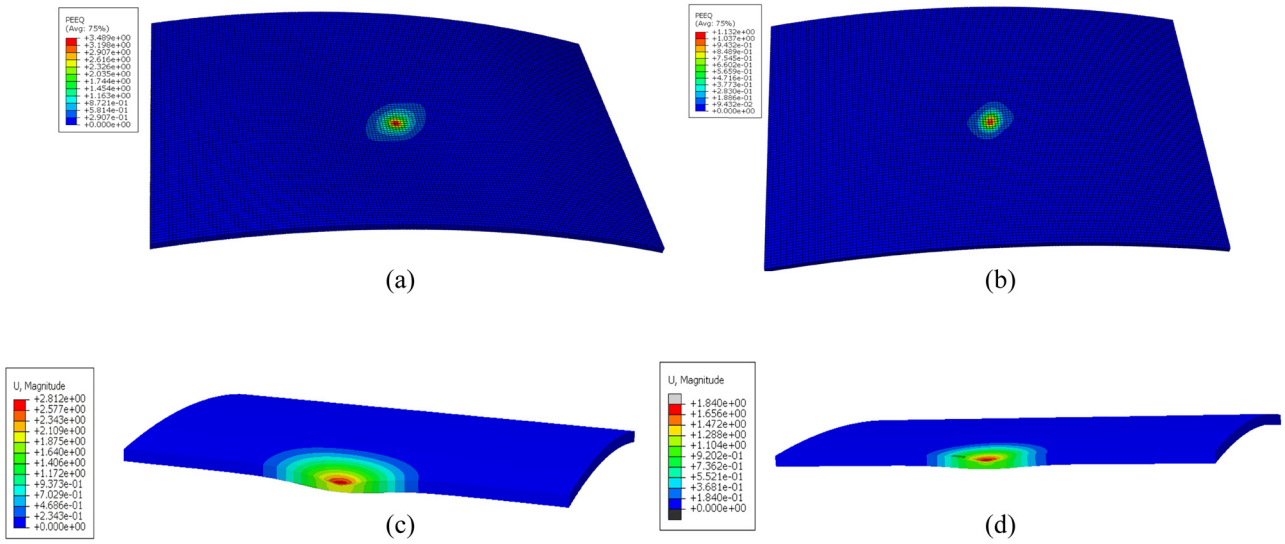

Figure 7: Contour graph of plastic deformation and displacement deformation of sandwich foam before and after optimization of sandwich skin: (a) plastic deformation of structural foam of YHR, (b) plastic deformation of structural foam of YH3, (c) YHR sandwich panel displacement, and (d) YH3 sandwich panel displacement.

11,268 mJ, respectively. The overall energy absorbed by the structure without optimization was the most, indicating that the overall damage was the most serious. From the perspective of damage dissipation energy, the energy value of YHR was the largest, reaching about 5.5 J, while the damage dissipation energy of the other three kinds of optimized structures gradually decreased to about 2.9 J, indicating that the damage of the upper panel of the non-optimized laminated structure was the most serious, and the damage of the upper panel of the YH3 laminated structure was light, with the best effect. The plastic dissipation energy of the four kinds of structures was similar, indicating that the sandwich foam was compressed and destroyed during the impact process. The comparison of energy response showed that in the laminate structure, the composite sandwich with [(0°,90°)] laminate structure as a whole absorbs the most energy and causes the most serious damage, while increasing the proportion of [±45°] laminate in the laminate structure can reduce the energy absorbed by the panel damage.

Figure 9(a) and (b) shows the impact force–time response curves and impact velocity–time response curves of the four ply structures before and after optimization. Under the impact energy of 20 J, the peak value of impact force and impact time of the four ply structures was close, which was due to the smaller size of the impact area relative to the overall structure, and the thickness of each structure was the same. From the impact force–time response curve, it can be seen that the peak value of YHR without optimization was the highest, and the maximum impact force was 4,438 N. The maximum impact force of YH1, YH2, and YH3 in the optimization scheme was 4,315, 4,236, and 4,182 N, respectively. The greater the impact force, the more serious the damage of the composite sandwich panel, and the impact force of the YH3 ply-optimized structure was the smallest and the damage was lighter. From the impact velocity–time response curve of the punch, the rebound velocity of the punch indirectly represents the energy, *i.e.*, the greater the rebound velocity, the greater the kinetic energy, the smaller the overall energy absorption, and the lighter the damage. The smaller the rebound velocity, the smaller the kinetic energy, the greater the overall energy absorbed, and the more serious the damage. The punch velocity of the non-optimized YHR structure was 1.465 m/s, while the punch velocity of the three optimized structures were 1.744, 1.954, and 1.982 m/s, respectively. The YHR velocity was far less than YH3 velocity, indicating that the damage of the upper panel of YHR was the most serious, while the damage of YH3 was the least. The two kinds of response curves showed that increasing the ratio of [±45°] ply in the laminated structure can reduce the impact force of the composite panel and punch during the impact process and slow down the damage caused by impact.

4.3 Impact damage results

After the impact, the upper surface of the sandwich panel showed different degrees of damage, while the lower panel showed no damage. From the results of finite element numerical calculation, the damage of the sandwich panel was mainly in the peripheral area of the contact punch, so

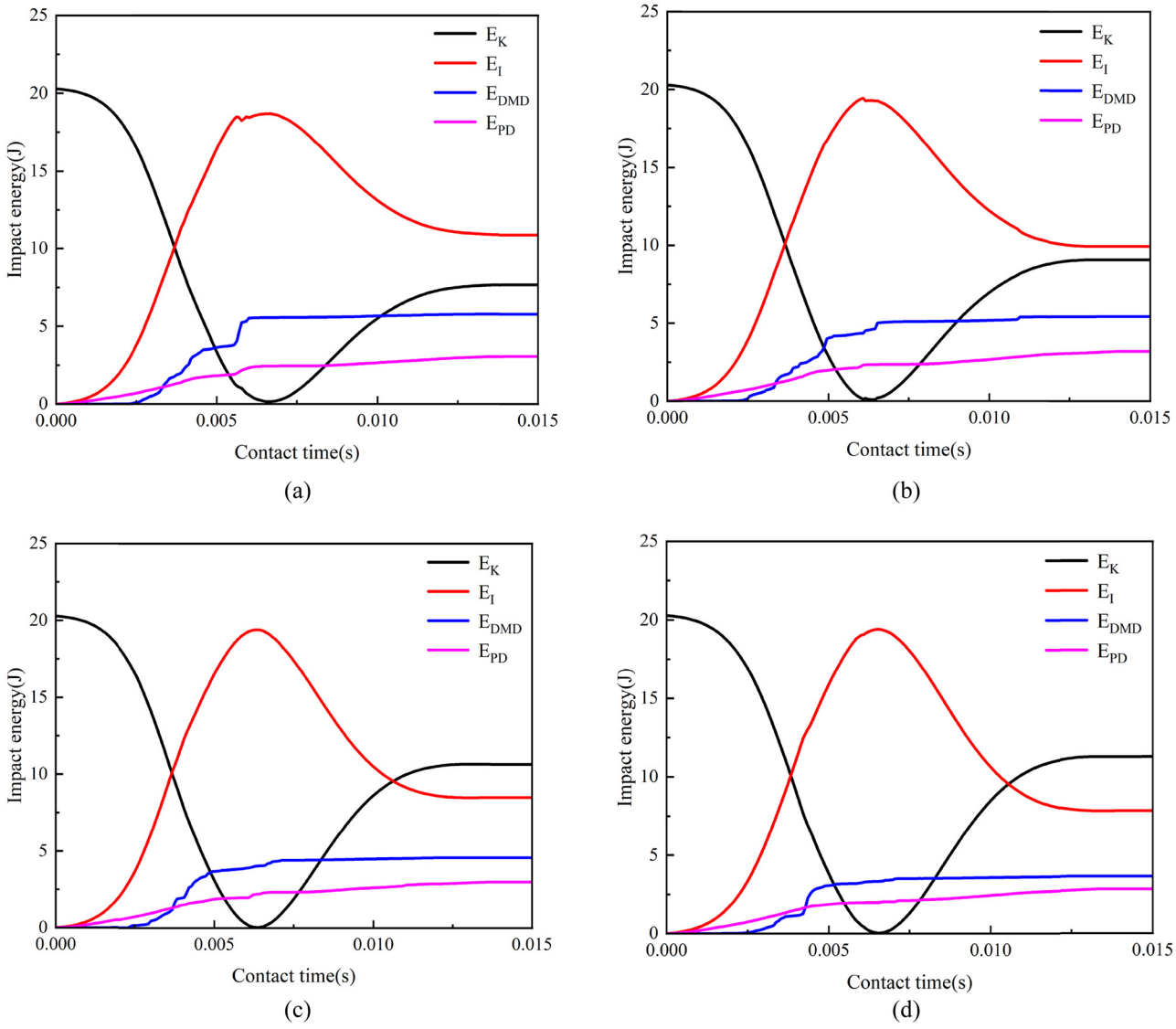

Figure 8: Energy response curve before and after optimization: (a) YHR energy response curve, (b) YH1 energy response curve, (c) YH2 energy response curve, and (d) YH3 energy response curve.

it was necessary to focus on the damage status of the size area near the impact point. The four damage conditions were fiber tensile failure (DAMAGEFT), fiber compression failure (DAMAGEFC), matrix tensile failure (DAMAGEMT), and matrix compression failure (DAMAGEMC). Different colors in the figure represent the damaged areas and damage conditions, where blue indicates that no damage occurs, which does not meet the damage law, and the red indicates that the damage law is met and the damage occurs, and the other colors represent incomplete damage.

The damage of the upper panel was mainly destroyed under low-energy impact, but the lower panel also tends to bear the impact load transferred from the upper panel. The damage of the upper panel was mainly destroyed under low-energy impact, but the lower panel also tends to bear the impact load transferred from the upper panel, which may cause a certain degree of damage. Although these damages were invisible to the naked eye, they also affect the overall impact resistance more or less. The damage type of the lower panel was consistent with that of the upper panel. The lower panel did not directly contact with the impact object, and there was energy absorption between the upper panel and the sandwich foam, so the impact response transferred to the lower panel was relatively low. Therefore, the main damage type was matrix tensile. Table 6 shows the tensile damage of the lower panel matrix under the four lamination structures before and after optimization. As can be seen from the table, the

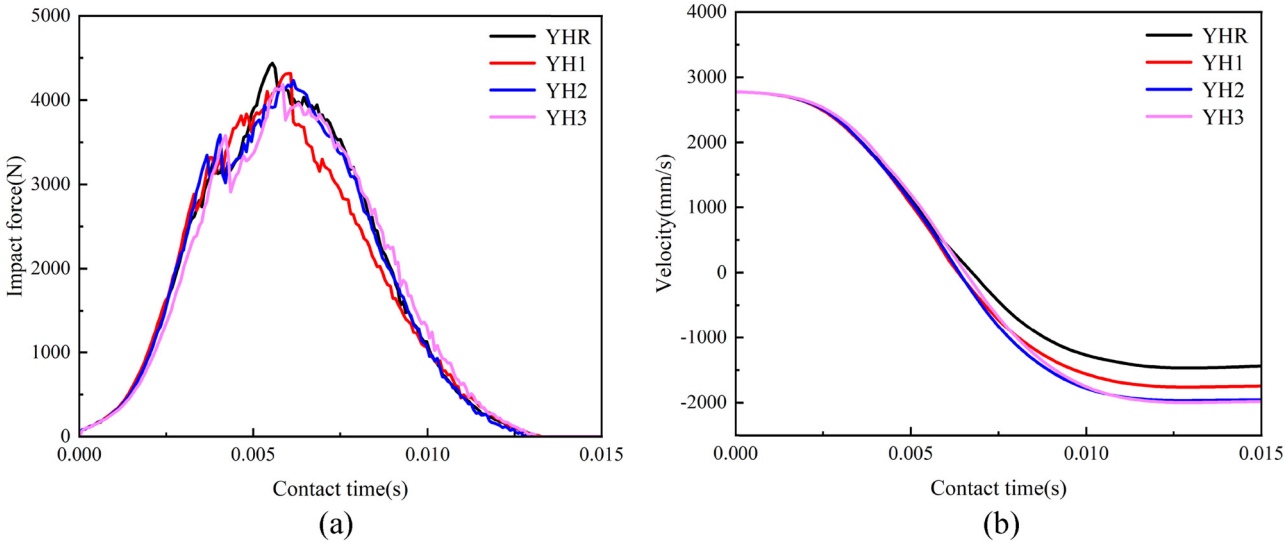

Figure 9: Response curve of impact force and velocity: (a) time response curve of impact force before and (b) time response curve of impact velocity.

tensile damage of the lower panel matrix mainly occurs in the lamination far away from the foam. Different from the tensile damage of the upper panel matrix, the tensile damage of the lower panel matrix was mainly elliptical and distributed in the central area. The damage area of the first layer of YHR before optimization was the largest,

Table 6: Tensile damage of lower panel matrix of each ply structure

	YHR	YH1	YH2	YH3
First ply				
Second ply				
Third ply				
Fourth ply				
Fifth ply				
Sixth ply				

while the YH1 changed the first two layers of the lamination to [±45°] lamination, and the damage area increased, and the following layers were all damaged. The matrix tensile damage area under the YH3 lamination structure was the smallest, indicating that the damage response of the lower panel using [±45°] lamination structure in the lamination was the lowest, and the impact resistance was the best.

5 Conclusion

Based on the impact mechanics testing, nondestructive testing, and finite element analysis of a sandwich structures with different ply forms, the aircraft fuselage skin structure was optimized and analyzed. For the sandwich panel with the same ply, with the increase of impact energy, the damage surface diameter of the upper panel increases, and the impact pit depth increases; under the same impact energy, increasing the number of plies of the panel can effectively slow down the expansion of the impact load in the layer and reduce the diameter of the damaged surface. At the same time, the damage diameter can be reduced by using symmetrical ply structure; adding [(0°,90°)] in the ply will increase the depth damage and reduce the impact performance of the sandwich panel, while adding [±45°] in the ply can greatly reduce the depth damage and surface damage range of the sandwich panel and improve the impact performance of the sandwich panel. Moreover, combined with the Hashin failure criterion, a finite element equivalent model was established. The load predicted by the numerical model was close to the measured value. Within a 10% margin of error, the bearing capacity of various panels is successfully predicted.

On the other hand, the absorption of impact energy was related to the damage degree of sandwich structure, and the more energy absorbed, the more serious the damage. Under the same impact energy, the thicker the sandwich panel, the higher the impact force, and the lower the energy conversion rate. Increased [(0°,90°)] ply in the composite panel could not only increase the damage degree in the tensile direction of fiber and matrix, but also increase the damage in the compressive direction; increased [±45°] ply can improve the bearing capacity of sandwich panels and reduce the energy absorbed by the failure of sandwich panels. For aircraft skin structure design, when the fuselage skin composite foam sandwich structure of a general-purpose aircraft was impacted by energy, the impact damage mainly concentrated in the area contacting the punch, the fiber fracture loss shape was mainly long strip, and the matrix fracture damage shape was ellipsoid, which was symmetrically distributed along the impact area. Increasing the proportion of [±45°] symmetrical ply in the structure can reduce the impact force borne by the structure, reduce the damage scope of the fuselage skin, and improve the impact resistance of the fuselage skin.

Funding information: Authors state no funding involved.

Author contributions: All authors have accepted responsibility for the entire content of this manuscript and consented to its submission to the journal, reviewed all the results and approved the final version of the manuscript. KY: Methodology, formal analysis. YY: Methodology, formal analysis, investigation. JW: Writing – original draft. XF: Writing – review and editing, supervision. DH and ZL: Formal analysis.

Conflict of interest: Authors state no conflict of interest.

Data availability statement: The authors claim that the data that support the findings of this study are available from the corresponding author upon reasonable request.

References

[1] Das TK, Ghosh P, Das NC. Preparation, development, outcomes, and application versatility of carbon fiber-based polymer composites: a review. Adv Compos Hybrid Mater. 2019;2:214–33.
[2] Li D-H, Yang F-T, Ma H-T, Deng L-D. Structural optimization and experimental verification of composite wing of electric aircraft based on aeroelastic load. Sci Technol Eng. 2020;20(18):7516–23.
[3] Castanie B, Bouvet C, Ginot M. Review of composite sandwich structure in aeronautic applications. Compos Part C: Open Access. 2020;1:10004.
[4] Vlach J, Doubrava R, Růžek R, Raška J, Horňas J, Kadlec M. Strain-field modifications in the surroundings of impact damage of carbon/epoxy laminate. Polymers. 2022;14(16):3243.
[5] Hu C, Huang G, Li C. Experimental and numerical study of low-velocity impact and tensile after impact for CFRP laminates single-lap joints adhesively bonded structure. Materials. 2021;14(4):1016.
[6] Tarlochan F. Sandwich structures for energy absorption applications: a review. Materials. 2021;14(16):4731.
[7] Bragagnolo G, Crocombe AD, Ogin SL, Sordon A, Mohagheghian I. Flexural behaviour of foam cored sandwich structures with through-thickness reinforcements. J Compos Sci. 2023;7(3):125.
[8] Barzkar A, Ghassemi M. Electric power systems in more and all electric aircraft: a review. IEEE Access. 2020;8:169314–32.
[9] Sarlioglu B, Morris CT. More electric aircraft: review, challenges, and opportunities for commercial transport aircraft. IEEE Trans Transp Electrif. 2015;1:99–64.
[10] Huang J, Yang FT. Development and challenges of electric aircraft with new energies. Acta Aeronaut Astronaut Sin. 2016;37(1):57–68.

[11] Stautner W, Ansell PJ, Haran KS. CHEETA: an all-electric aircraft takes cryogenics and superconductivity on board: combatting climate change. IEEE Electrif Mag. 2022;10(2):34–42.
[12] Yang FT, Fan ZW, Xiang S, Liu Y, Zhao W. Technical innovation and practice of electric aircraft in China. Acta Aeronaut Astronaut Sin. 2021;42(3):624–19.
[13] Yancey RN. Challenges, opportunities, and perspectives on lightweight composite structures: aerospace versus automotive. Lightweight Compos Struct Transp. 2016;1:35–52.
[14] Huo X, Liu H, Luo Q, Sun G, Li Q. On low-velocity impact response of foam-core sandwich panels. Int J Mech Sci. 2020;181:105681.
[15] Wang J, Li J, GangaRao H, Liang R, Chen J. Low-velocity impact responses and CAI properties of synthetic foam sandwiches. Compos Struct. 2019;220:412–22.
[16] Yang K, Gong P, Yang L, Zhang L, Zhang Z, Ma G. The effect of different structural designs on impact resistance to carbon fiber foam sandwich structures. e-Polym. 2021;22(1):12–8.
[17] Yang K, Yang L, Gong P, Zhang L, Yue Y, Li Q. Experiment and analysis of mechanical properties of carbon fiber composite laminates under impact compression. e-Polym. 2022;22(1):309–17.
[18] Taraghi I, Fereidoon A. Non-destructive evaluation of damage modes in nanocomposite foam-core sandwich panel subjected to low-velocity impact. Compos Part B: Eng. 2016;103:51–9.
[19] Sun G, Huo X, Chen D, Li Q. Experimental and numerical study on honeycomb sandwich panels under bending and in-panel compression. Mater Des. 2017;133:154–68.
[20] Kim BJ. Characteristics of joining inserts for composite sandwich panels. Compos Struct. 2008;86(1–3):55–60.
[21] Mines RAW, Worrall CM, Gibson AG. Low velocity perforation behaviour of polymer composite sandwich panels. Int J Impact Eng. 1998;21(10):855–79.
[22] Samlal S, Santhanakrishnan R. Low-velocity impact behavior of foam core sandwich panels with inter-ply and intra-ply carbon/kevlar/epoxy hybrid face sheets. Polymers. 2022;14(5):1060.
[23] Huo X, Liu H, Luo Q, Sun G, Li Q. On low-velocity impact response of foam-core sandwich panels. Int J Mech Sci. 2020;181:105681.
[24] Zhu K, Zheng X, Peng J, Sun J, Huang R, Yan L. The relationship between the impact position interference and CAI strength of composite sandwich structures under double impacts. Compos Part B. 2024;268:111092.
[25] Xiao W, Li Y, Hu Y, Song Z, Cai W, Li X. Analytical study on the dynamic mechanical behaviours of foam-core sandwich plate under repeated impacts. Thin-Walled Struct. 2024;196:111480.
[26] Li J, Zhang W, Wang Z, Wang Q, Wu T, Qin Q. Dynamic response, and failure of CFRP Kagome lattice core sandwich panels subjected to low-velocity impact. Int J Impact Eng. 2023;181:104737.
[27] Valerio A, Mauro Z, Aniello R. Experimental and numerical assessment of the impact behaviour of a composite sandwich panel with a polymeric honeycomb core. Int J Impact Eng. 2023;171:104392.
[28] Besant T, Davies GAO, Hitchings D. Finite element modelling of low velocity impact of composite sandwich panels. Composites Part A. 2001;32(9):1189–96.
[29] Sun G, Wang E, Wang H, Xiao Z, Li Q. Low-velocity impact behaviour of sandwich panels with homogeneous and stepwise graded foam cores. Mater Des. 2018;160:1117–36.
[30] Zhou J, Guan ZW, Cantwell WJ. The impact response of graded foam sandwich structures. Compos Structure. 2013;97:370–7.
[31] Zhu Y, Sun Y. Low-velocity impact response of multilayer foam core sandwich panels with composite face sheets. Int J Mech Sci. 2021;209:106704.
[32] Binbin L, Jianwu Z, Ying L, Panding W, Li X, Ruxin G, et al. Damage accumulation mechanism of composite laminates subjected to repeated low velocity impacts. Int J Mech Sci. 2020;182:105783.